LARGE-SCALE MEASUREMENTS AND NUMERICAL SIMULATIONS OF IN-CLOUD ICING AROUND THE RIDGE OF A MOUNTAIN PEAK

Magne A. Drage
UNIS/UIB

Thomas K. Thiis
Norwegian Building Research Institute

ABSTRACT: Atmospheric icing by in-cloud icing has been measured around the ridge of Mt. Gaustatoppen (59°51', 08°N39'E, 1882 m a.s.l.) in Norway, during a 5-day period. Sixteen sticks of 2 m height and 3 cm diameter were placed around the edge of the mountain ridge. A finite volume CFD (Computational Fluid Dynamics) solver was used to simulate the wind flow and the rate of icing around the top 270 meters of the mountain.
Measurements and simulations show that even small variations in the location of the sticks around the ridge of a mountain peak, can cause large variations in accreted ice on the sticks. A basic understanding of the air flow around isolated mountain peaks is vital to understand how complex topography and altering wind direction can influence icing intensity. In this case, use of a micro scale numerical model to describe the wind field around the mountain peak, or measurements at the location for a short time period, proved to give valuable information. A study of the icing around a building located at the peak indicate that local sheltering may reduce the in cloud icing by up to 100 %.

1. INTRODUCTION

In regions with severe climatic conditions, the planning and building of new constructions calls for special attention to be paid with respect to atmospheric icing. In many cases the most severe form of icing is in-cloud icing, especially in elevated areas. The expected maximum amount of in-cloud icing is an important design criterion within the building industry, communications and energy distribution. The largest recorded iceload on a power line is 305 kg m^{-1}. This was measured on a 22kV overhead line close to the Norwegian village Voss in 1961 (Makkonen, 2000). In general, it has not been the practice to collect ice data before a construction is erected in an environment favourable of in-cloud icing. This can often result in operational

problems and failures, as shown by the collapse of 13 TV towers in the United States alone due to ice loads during a 20-year period (Sundin and Makkonen, 1998). A power line in western Norway, which experienced serious icing and failure, was re-erected in a parallel section 48 m lower than the original line. The new line was almost completey sheltered against icing by the hill above (Raastad, 1958). In this context, the location of the construction on a mountain peak or slope is of great importance since icing is strongly dependent upon wind speed, wind direction, cloud liquid content and cloud droplet spectra. Full scale measurements of icing are sparsely reported. The main features can be recognised in wind tunnel experiments, but such experiments suffer from scaling problems and a lack of information in connection with local variations of climatologically parameters.

In-cloud icing, which is the main process studied in this field measurement program, occurs when super cooled cloud droplets collide with a surface and freeze spontaneously. This is the type of icing which gives the highest accumulated ice load on structures (Makkonen and Ahti, 1995). The rate of icing onto an object by in-cloud icing by dry growth is given by the equation

$$\frac{dM}{dt} = \alpha_1 \alpha_2 \alpha_3 \cdot q_{LWC} \cdot A \cdot V \quad [\text{Kg·s}^{-1}] \quad\quad (1)$$

where q_{LWC} is the liquid water content of the air, flowing with the wind speed velocity V, towards the cross-sectional area A, of the object. The efficiency coefficient α_1 represents the collision efficiency, which is the fraction of the total droplets in the path of the object that collide with the object, given by Finstad et al. (1988a) and Makkonen and Stallabras (1987). Small droplets, large cross sections and low wind speeds reduce α_1. α_2 and α_3 represent the collection and accretion efficiency, respectively. They are assumed to be equal to 1 for in cloud icing, according to earlier field measurements by, for example, Ahti and Makkonen (1982) and Sundin and Makkonen (1998).

The meteorological input parameters in eq.1 are liquid water content (LWC), air temperature and wind speed. Measurement of these parameters does not normally exist at any actual icing site, making reliable estimates crucially important. The method for calculating these estimates are given by Harstveit (2002) and Drage and Hauge (2004).

Estimates in this study were made using measurements from Gaustatoppen over a one-year period. These estimates suggested a temperature gradient for dry conditions γ_d = 0.86 ºC/100m, and a temperature gradient for wet conditions γ_w = 0.52 ºC/100m, with standard deviations of 0.16 and 0.11,

respectively. The air temperature at cloud base T_c was found solving by iteration the analytical approximation given by:

$$T_c = B / \ln \left[\frac{A\varepsilon}{wp_1} \left(\frac{T_1}{T_c} \right)^{1/k} \right] \qquad (2)$$

where A, B, *k* are constants, respectively $2.53 \cdot 10^8$ kPa, $5.42 \cdot 10^3$ K and 0.286. w, T_1, and p_1 are mixing ratio, air temperature and air pressure known at an unsaturated lower level 1(subscript 1) (Rogers and Yau, 1989). Furthermore, the cloud base height was estimated by using the temperature gradients defined above, either by following the gradient for unsaturated conditions from below, or by following the gradient for saturated conditions from above. By measuring air temperature and relative humidity at level 1 below cloud base, it is possible to estimate the liquid water content (LWC) of the cloud a certain height above the cloud base. This method is described by Drage and Hauge (2004):

$$\rho_{LWC} = \varepsilon \cdot \rho_{d2} \left(\frac{e_1}{p_1} - \frac{e_2}{p_2} \right) \qquad (3)$$

with the cloud base lying between the lower (subscript 1) and upper (subscript 2) levels. The constant ε is the ratio of the molecular weight for water vapour and dry air, equal 0.622. The density of dry air at level 2 is given by ρ_{d2}. The water vapour pressure and the air pressure at the two levels are given by e_1, e_2 and p_1, p_2 respectively. This equation is based upon the assumption that the total water content of the air is constant with height.

According to Sundin and Makkonen (1998), icing is forecasted when the air temperature is below 0 ºC and the relative humidity is higher than a critical value, or that the cloud base is below the level of the site in interest. Furthermore, the icing intensity is simply assumed to be a function of the wind speed.

However, literature shows convincing evidence that LWC increases with height in a cloud layer. This increase in LWC is accounted for by an increase in droplet size rather than droplet concentration. In fact, droplet concentration is observed to be approximately constant throughout a stratus cloud layer, whereas droplet size increases monotonically with height (Rogers and Yau, 1989). Assuming a constant droplet concentration, droplet size is only a function of LWC, which increases with height above the cloud base. Given a LWC dependent upon height above cloud base in eq. 3, it is now possible to estimate the icing intensity onto a structure given in eq. 1 as a function of height above sea level. These calculations also require estimates of wind speed and collision efficiency.

A Computational Fluid Dynamics (CFD) three-dimensional solver, described in the next chapter, calculates the local wind speed and the icing rate. The collision efficiency in eq. 1 is dependent upon wind speed, diameter of the structure (cylindrical), and median volume droplet diameter (Finstad et al. 1988b). Assuming a constant droplet concentration, the mean volume droplet diameter is calculated as a function of height above the cloud base.

During icing with approximately constant wind direction, the ice will form an ice vane towards the wind, in which case the theory for a cylinder discussed above is generally inapplicable. One approach to this problem is to plot the icing intensity for varying cylinder diameters. In this theoretical case an LWC of 0.4 g/m3 and a wind speed of 10 m/s were chosen, and four cases of different droplet concentration have been plotted (figure 1). Measurements and observations during the icing incident studied here showed that the ice vane created a peak towards the wind. The width of the peak was observed to decrease as the ice vane grew. This can be interpreted as a decreasing effective cylinder diameter as the icing continues. Applying the equations by Finstad et al. (1988a) and assuming a droplet concentration of 10 E+7 (m3) and an initial cylinder diameter of 3 cm, figure 1 shows that the icing intensity decreases rapidly when the effective cylinder diameter decreases below 0.02 m.
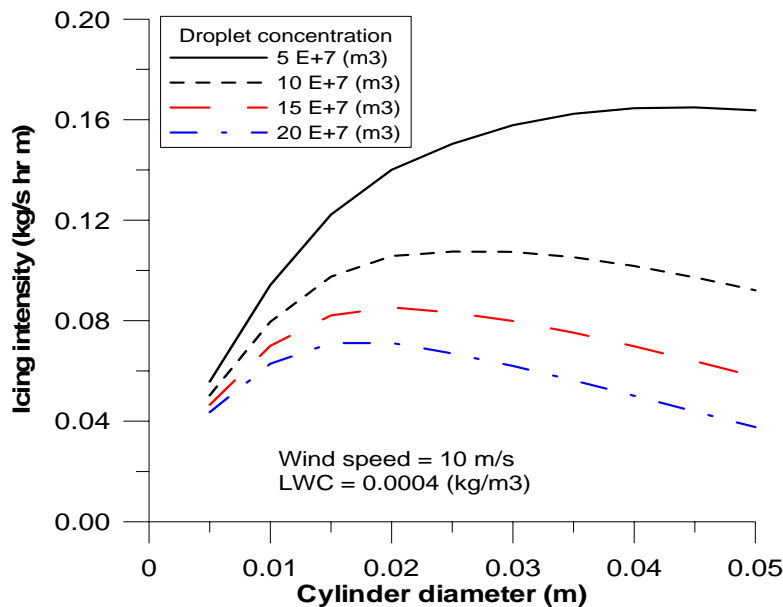

Figure 1. Theoretical icing intensity on a cylinder with varying cylinder diameter. Wind speed and LWC are 10 m/s and 0.4 g/m3, respectively. The computations are based upon the equations given by Finstad et al. (1988a).

2. STUDY SITE AND METHODS

The field experiment was performed at the mountain Gaustatoppen, Telemark, Norway. The mountain has a peak of 1883 m a.s.l. and a SE-NW leading ridge (figure 2). The mean level of the terrain surrounding the mountain within a distance of 10 km is estimated to be approximately 950 m a.s.l. The peak is exposed to rather harsh climatic conditions, with a mean annual air temperature of -4.3 ºC. It experiences 177 days per year with wind speeds stronger than 10 m s^{-1} and 14 days per year stronger than 20 m s^{-1}. The peak is exposed to heavy icing in all wind directions except from a northerly direction. The maximum ice load on a horizontal rod exposed at the peak has been measured to 284 kg/m (Finstad et al. 1988c).

2.1 Measurements

The experiment lasted for 5 days from March 28 to April 2, 2003, which was a sufficient length of time to form significant ice accretion on the sticks. The accumulated precipitation at the nearby synoptic station of Møsstrand was measured to 6.7 mm during the experiment. This station is operated by the Norwegian Meteorological Institute, and is located 977 m a.s.l. 31 km west of the mountain peak.

To study variation of icing in the terrain, sixteen sticks of 2 m height and 3 cm diameter were placed around the edge of the mountain ridge, from an altitude of 1745 to 1845 m.a.s.l (figure 3). The sticks were placed such that one profile was along the ridge of the mountain (hereafter profile 1), and two profiles were perpendicular to the ridge of the mountain (hereafter profile 2 (upper) and profile 3 (lower)). The distance in the terrain between the sticks following a profile was 40 meters. The accreted ice on the sticks was measured two times during the experiment. The length of the ice vane at 0.10, 0.65, 1.30 and 2.00 meters above the terrain was measured along with the total weight of accreted ice (figure 4).

An attempt of measuring wind speed and wind direction was performed by applying a heated sonic anemometer at 1800 m a.s.l. Icing onto the transducers caused irregularities in the wind speed data set, and a filtering of these data was therefore necessary. A supplement of data from handheld anemometers and from HIRLAM10 (High Resolution Limited Area Model 10km) was also included in the data set.
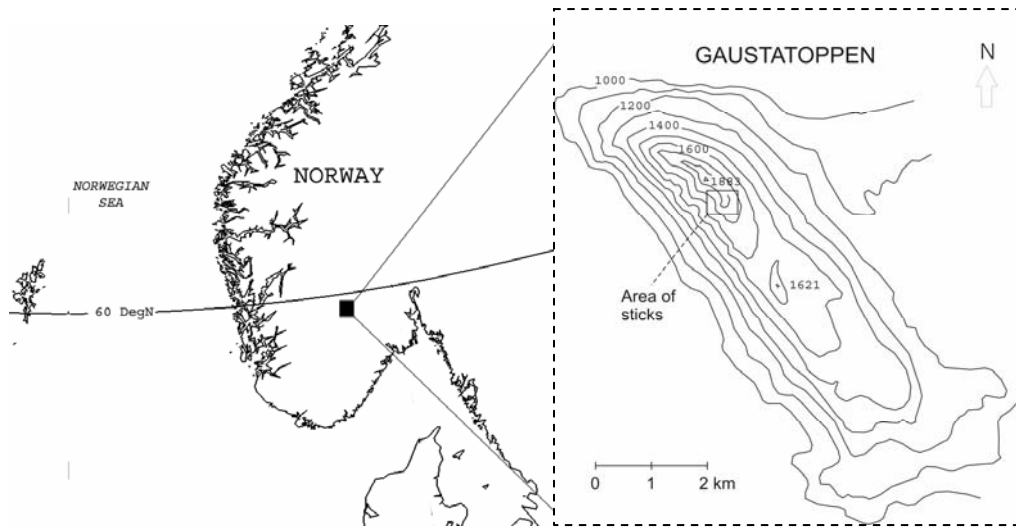
Figure 2. Location of the mountain Gaustatoppen (59º51´N, 08º39´E), 1883 meter above sea level in southern Norway.
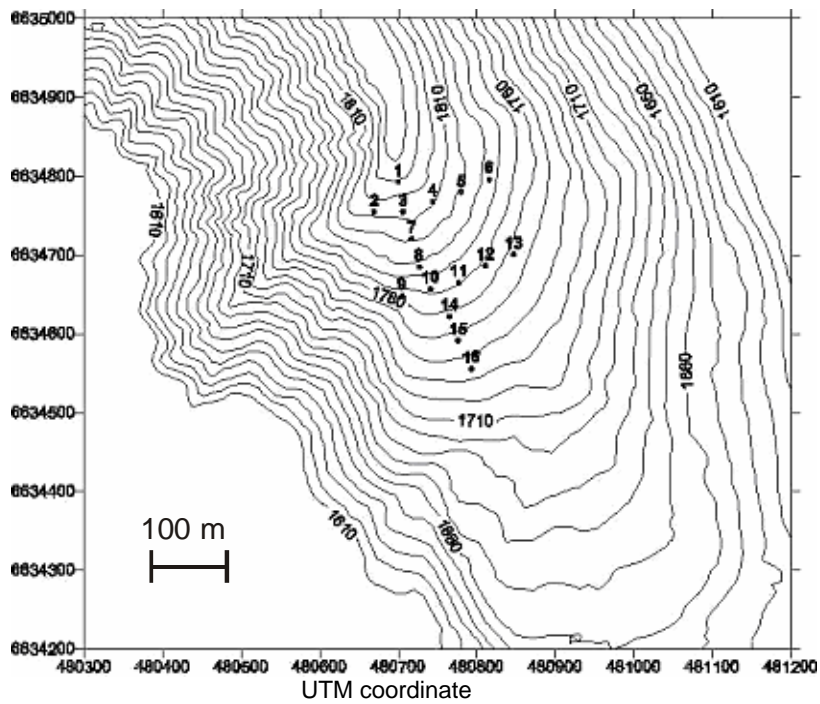

Figure 3. Topography plot of stick location around the southern ridge of the mountain Gaustatoppen. The equidistance is 10 m.

The data from the weather station at Møsstrand was included for determining the large-scale wind direction during the field experiment. Measurements at this station are taken daily at 0700 hrs, 1300 hrs and 1900 hrs GMT.

The accumulated precipitation for 12-hour periods is also measured everyday at 0700 hrs and 1900 hrs GMT. The analysis output data of wind speed and wind direction from the operational model HIRLAM10 at 850 hPa was also included as a supplement and verification to the meteorological data from the station at Møsstrand and as a basis for estimating the wind speed at Gaustatoppen 1800 m a.s.l.

In addition, a series of measurements by a Rotating Multi-Cylinder (RMC) were performed in order to estimate cloud liquid water content and median volume droplet size given by the method of Finstad et al (1988b). The icing onto the multicylinder was measured after six incidents of icing, each of 20 minute durations between 1000 hrs and 1400 hrs on April 1st. Based upon these measurements the average LWC at 1800 m a.s.l. was estimated to 0.48 (g/m3), with a standard deviation of 0.11 (g/m3). Using the weather station measurements from 1160 m a.s.l and the method described by Drage and Hauge (2004), the LWC at 1800 m a.s.l was estimated as 0.45 (g/m3), with a corresponding standard deviation of only 0.002 (g/m3).

Figure 4. Measurements of the length of the ice wane to the left, and a demonstration of a typical ice accretion on a stick to the right.

At the site, the temperature, humidity and wind speed were measured by four automatic weather stations along the mountain slope, located at 1811, 1540, 1298 and 1150 m a.s.l. The wind speed sensors were rotating cup anemometers. The sampling interval for all the equipment was ten minutes. In addition, the icing was measured on a one meter high rotating cylindrical rod with diameter 3 cm placed at 1800 m a.s.l. The rod was placed on a load cell which measured the ice load every 10 minutes (Drage and de Lange, 2005). The ice was distributed on the rod in a circular shape due to rotation, and the variation in the ice load with height was negligible (figure 5).

Figure 5. Ice accretion on the ice scale Apcril 1. 2003. The length of the rod is 1 m, and the diameter without ice is 3 cm.

2.2 Numerical simulations

A finite volume CFD solver (Cham inc., 2004) was used to solve the wind flow around the top 270 meters of the mountain. The Reynolds Averaged Navier—Stokes equations, closed with the RNG (ReNormalized Group theory) k-ε turbulence model were solved for a three dimensional cartesian grid (Yakhot et.al, 1992). The RNG model combines the eddy viscosity concept with the statistics of small-scale turbulence. The effects of small-scale turbulence are represented by means of a random forcing function in the Navier Stokes equation. The RNG procedure systematically removes the small scales of motion from the governing equations by expressing their effects in terms of larger scale motions and a modified viscosity (Versteeg and Malalasekera, 1995). The method is frequently used in the assessment of wind power turbine sites.

In this study, the grid size was 150x140x49 cells with grid refinement close to the area where the measurements were performed. Within this area, the grid size is 7x7x5 meters. To improve the accuracy of the flow simulation at the fluid/solid boundary, the Partial Solution Algorithm (PARSOL) was applied (Cham, 2004). This algorithm calculates the intersections of the mountain surface with the cell edges and ensures that the terms in the algebraic representations of the conservation equations are properly modified. The rate of icing was calculated for each cell with equation 1. The terrain model was constructed on the basis of map data with a 5 m equidistance. The roughness of the terrain is assumed to be 0.01 m (Stull, 1988). The flow solver has been used at two different wind episodes. Table 1 gives an overview of the simulation cases.

The wind direction applied in the model is considered to be constant during each experiment. Measurements and observations show that the wind direction is within ± 15 degrees during each experiment at the same time as the ice load is increasing according to the ice scale (figure 6). The wind speed applied in each simulation case is roughly estimated by measurements at Gaustatoppen at 1160 m a.s.l.

Table 1. Overview of the numerical simulation cases

Case no.	Wind direction [deg]	Wind speed [m/s]	Duration (hrs)
1	260	17,5	48
2	190	11,5	52

3. RESULTS

The temperature during this field experiment from March 28 to April 2 ranged from -2.4 ºC to –12.2 ºC. Based on this, all icing was assumed to be of the type in-cloud icing, according to existing models for estimating icing on structures (Sundin and Makkonen, 1998).

The accumulated ice on the sticks located around the southern ridge (figure 3) was measured after two incidents of icing (table 1). The first measurement period lasted 48 hours, from 1500 hrs March 28 to 1500 hrs March 30, while the second measurement period lasted 52 hours, from 1600 hrs March 30 to 2000 hrs April 1. The third icing incident that gave accretion of ice on the sticks around the building lasted 13.5 hours, from 2100 hrs April 1 to 1030 hrs April 2. Measurements from the Møsstrand synoptic weather station, situated 31 km to the west of Gaustatoppen, and results from the Hirlam10 model at 850 hPa showed a westerly wind during the first incident, a southerly wind during the second incident and a north-westerly wind during the third incident. The precipitation during the whole experiment was associated with the passage of two weather systems. Their passage is indicated in figure 6 by a period of no precipitation midway through the experiment.

To study the effect of a construction with respect to in-cloud ice, eight sticks were placed around a building at the peak, as described in figure 7a. The height of the building was 2.3 m, and the lengths of the walls were 2.5 and 3.5 meters. The ice accumulation on the sticks placed around the building was measured after the third icing incident (figure 7b). The sticks on the western and southern side of the building gave approximately the same amount of ice accumulation. A smaller amount was recorded on the northern side, and there was no accumulation at all on the eastern lee side. The distinct difference in the accumulation of ice on the sticks around the building illustrates how the rate of icing may vary considerably around a single location. Sticks 5 and 6 were on the leeward side to the south-east of the building and experienced no icing during the experiment, while sticks 3 and 4 on north-east side were partly in the lee zone, and therefore had reduced icing.
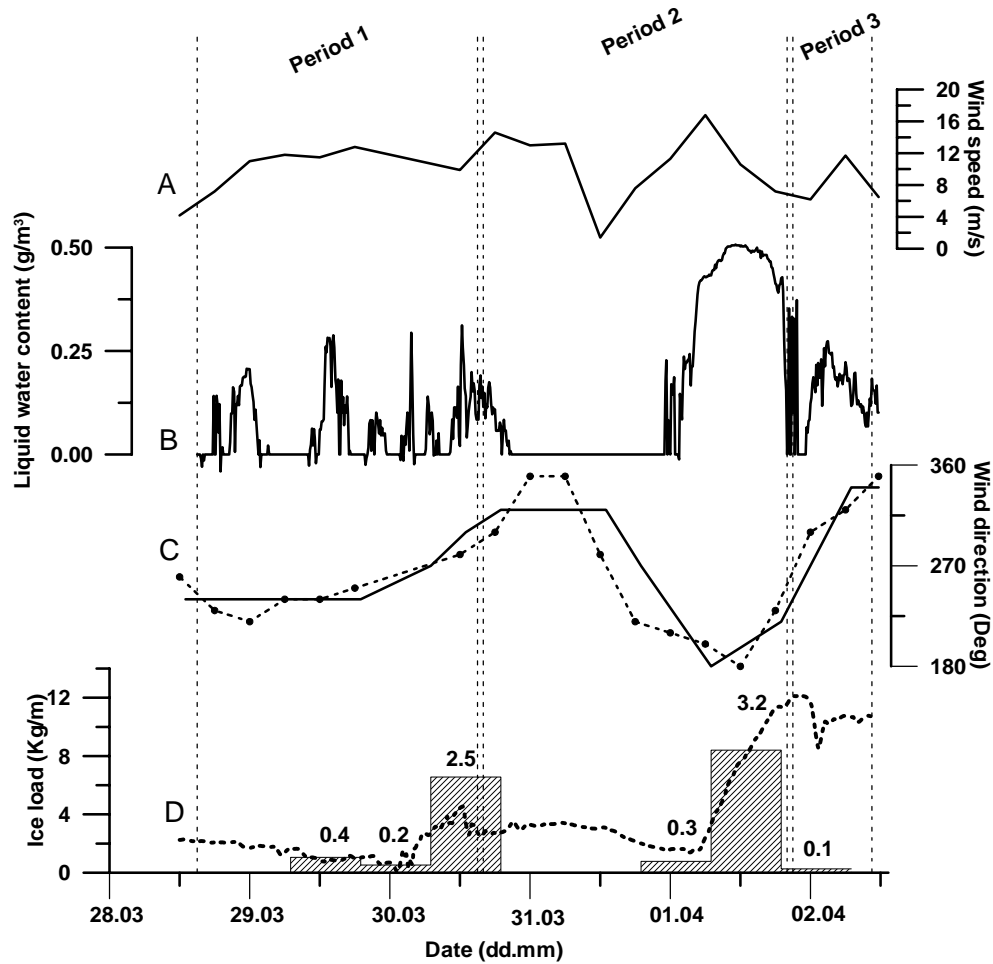
Figure 6. A. Simulated wind speed at 850 hPa in Hirlam10. B. Calculated LWC at 1800 m a.s.l. C. Wind direction at 850 hPa in Hirlam10 (dotted line with symbol) plotted against measured wind speed at Møsstrand. D. Measured ice load on the ice scale at 1800 m a.s.l. The step plot is measured 12hrs accumulated precipitation (mm) at Møsstrand, indicated by the numbers above the histograms.
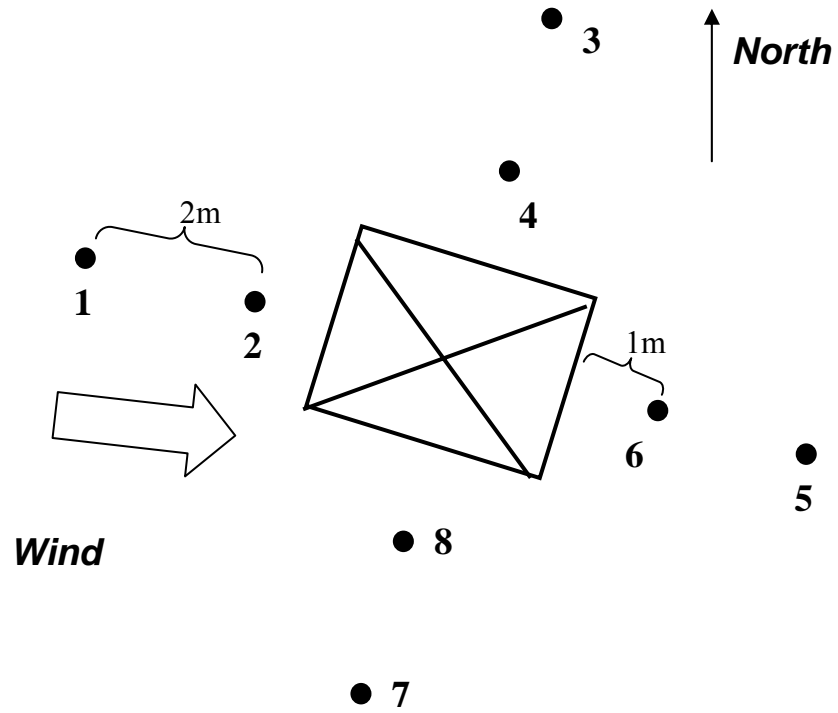
Figure 7a. Measurement-setup around the building at the mountain peak. The length, width and height of the building are, 2.5 m, 3.5 m and 2.3 m respectively.
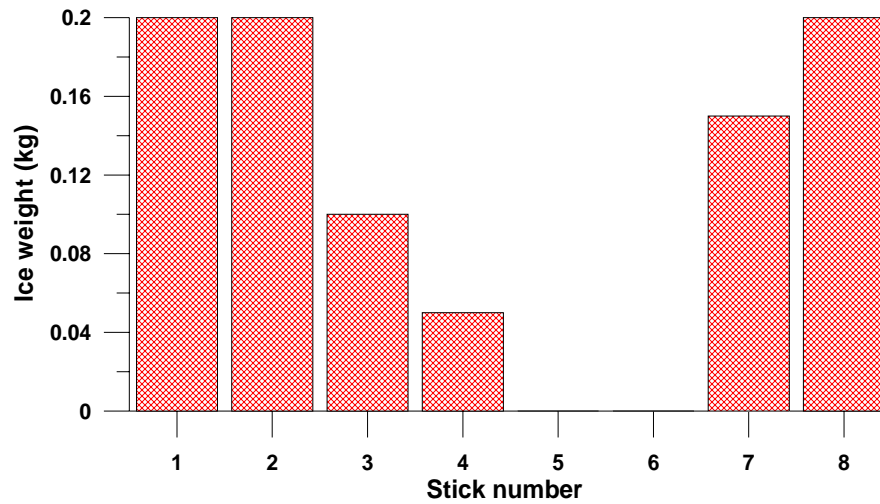

Figure 7b. Accumulated ice accretion on the sticks around the building.

Numerical simulations of the wind conditions during the actual icing incidents by the CFD solver, show strong local variations (figure 8). A normalization of the simulated surface wind at each stick to the inlet wind speed in the model, gives an indication of the relative change in wind speed related to location (figure 9). These wind speed ratios at each stick is considered constant through the experiments.
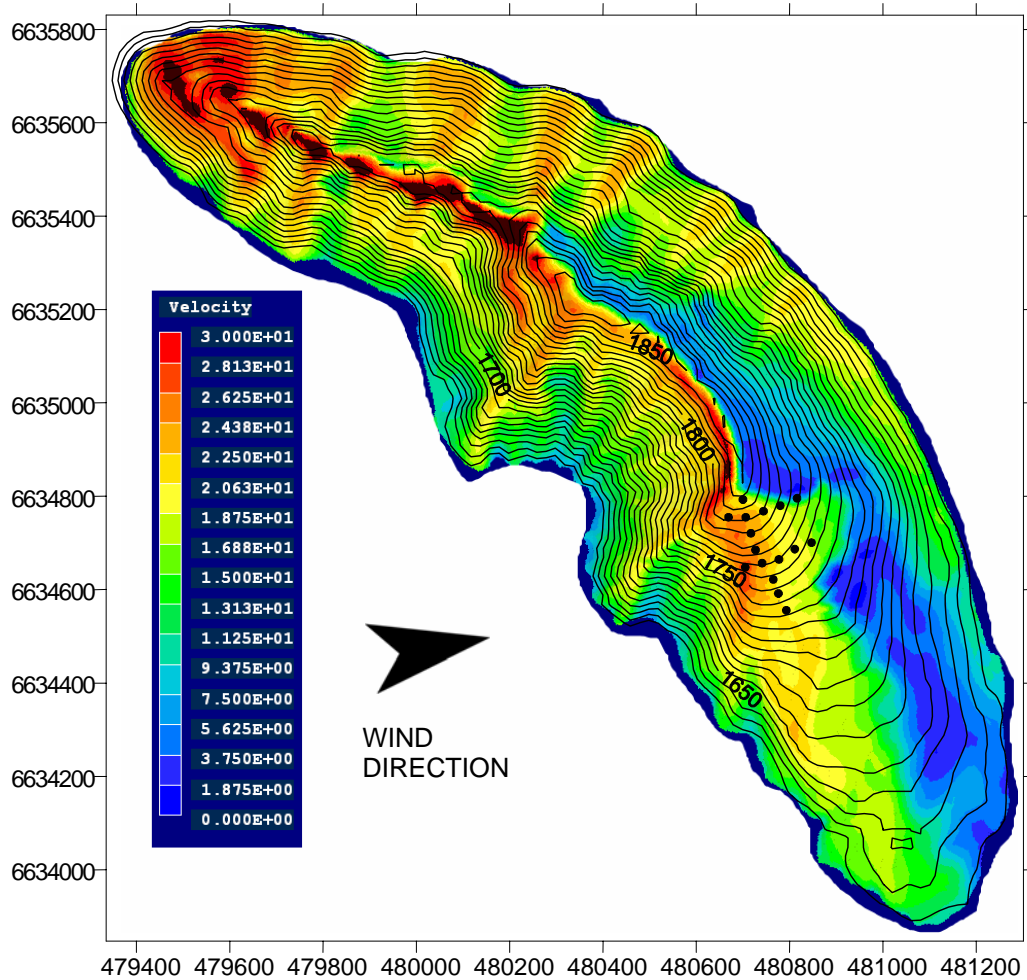

Figure 8. Simulated wind speed (m/s) in simulation case 1. Inlet wind speed is 17,5 m/s. The scales on the axis are in meter.
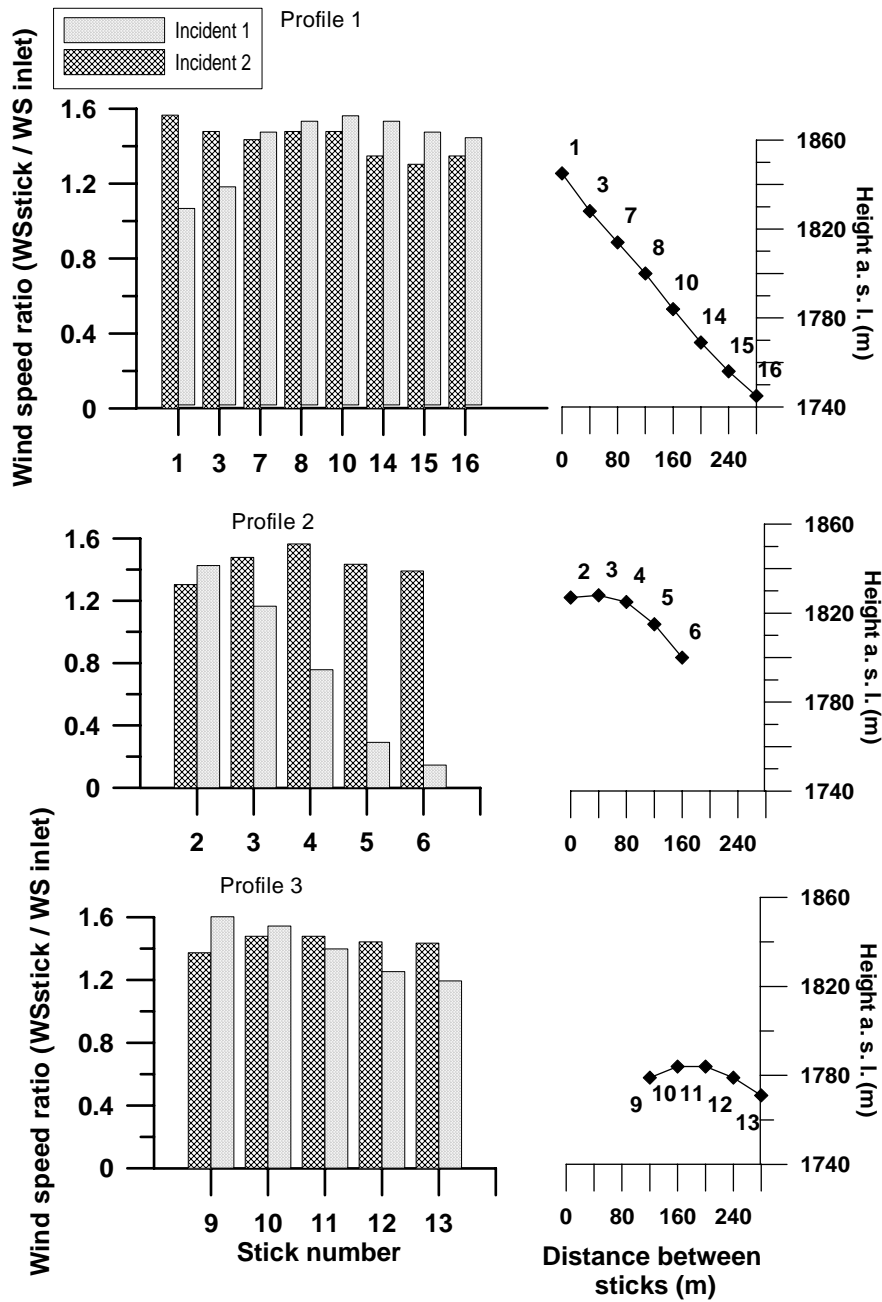
Figure 9. Simulated wind velocity ratio in the two different simulation cases. Location of the sticks related to height and horizontal distance is plotted to the left.
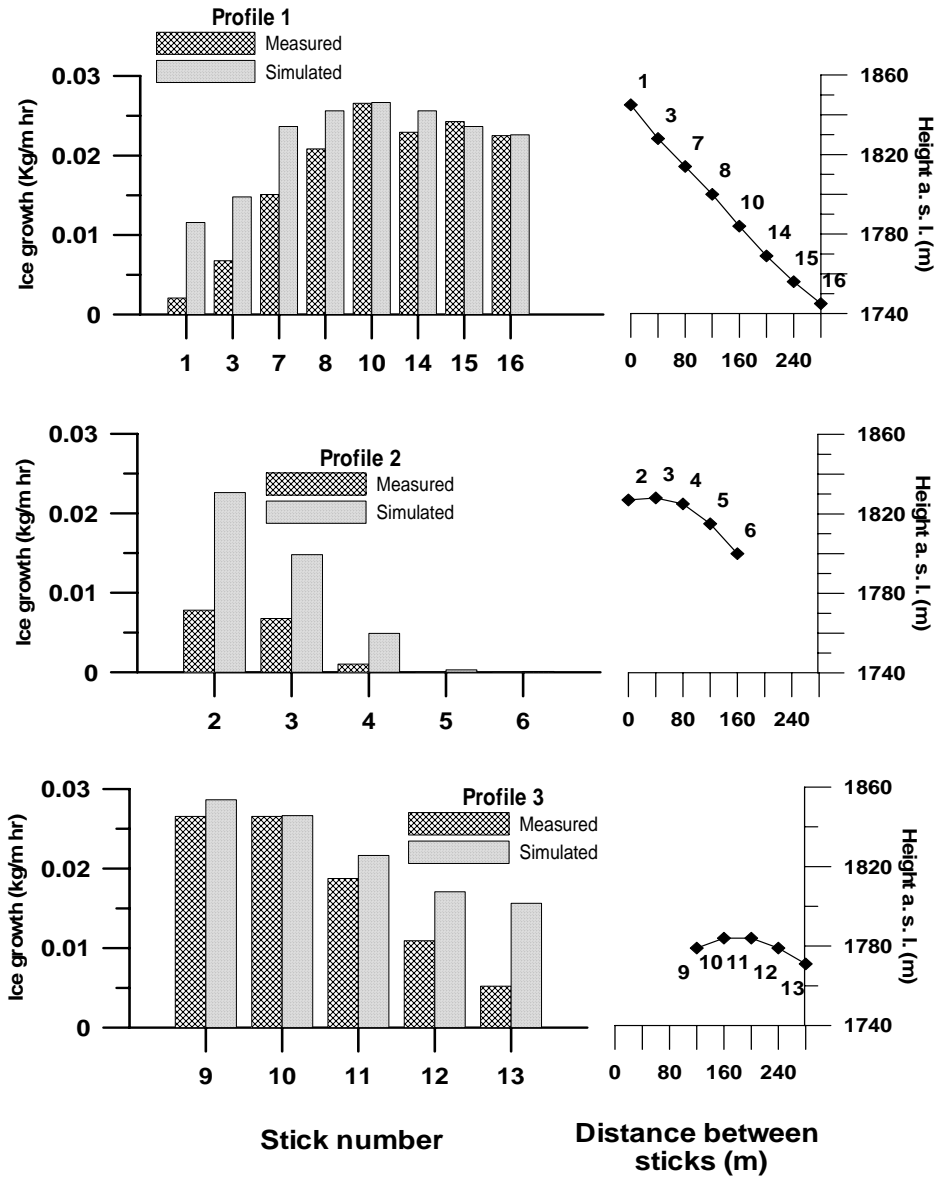
86

Figure 10. Plot of measured and estimated ice growth rate on each stick in the terrain during icing incident 1. Locations of the sticks related to height and horizontal distance is plotted to the left.

According to the model, during incident 1, with the winds from the west, there is an increase in wind speed at the ridge and a sharp decrease in winds speed on the leeward side. The wind speed increases with increasing height due to the forcing of the air masses around the ridge. Moving towards the leeward side gives a decrease in modelled wind speed of 90 % and a decrease in measured ice growth towards zero on sticks 5 and 6, indicated clearly by profile 2 (figure 10). With southerly winds, as during incident 2, there is no

such simulated speed up at the ridge, or any sharp decrease in wind speed at the leeward side of the ridge as in incident 1 (figure 9). A slight speed up at the ridge is most apparent in profile 2, while profile 3 shows approximately no variation. The last part of this study is concerned with the testing of the models presented in papers 2 and 3. Ice load data collected at Mt. Brosviksåta and Mt. Gaustatoppen during the winter 2003/2004 is evaluated.

During the first incident of icing, the measurements show a decrease in icing intensity with increasing height in profile 1, from 0.022 Kg m^{-1} hr^{-1} at stick 16, to 0.002 Kg m^{-1} hr^{-1} at stick 1 (figure 10). Likewise there is a decreasing trend in intensity from the west to the east side of the ridge. The measurement of the sticks in profile 2 and 3 gave maximum intensity for locations on the upstream-western side of the ridge, with 0.008 Kg m^{-1} hr^{-1} at stick 2, and 0.027 Kg m^{-1} hr^{-1} at stick 9. At the same time stick number 5 and 6 at the downstream-eastern side of the ridge of profile 2 had no accretion of ice, and stick 13 in profile 3 had 0.005Kg m^{-1} hr^{-1}.

Simulated icing intensity during incident 1 corresponds well with measured intensity (figure 10). The input parameters for this simulation were estimated LWC at 1800 m a.s.l given by the method by Drage and Hauge (2004). The wind speed was estimated at each stick by applying the wind speed ratio given by the CFD-solver, to the wind speed at 850 hPa in Hirlam10. LWC was estimated each ten minutes, while HIRLAM10 gave data only each six hours. A linear interpolation of wind speed to ten minute values was therefore performed. The droplet concentration was assumed constant with height above cloud base, equal to 113 cm^{-3}, given by Gjessing and Skartveit (1990). Furthermore, a calculation of the collision efficiency at each stick was performed using the method given by Finstad et al. (1988a) and assuming a constant cylinder diameter equal to 3 cm. The decreasing trend in icing intensity towards the east of profiles 2 and 3 can be identified in both the measurements and estimates (figure 10). An overestimate of icing intensity at stick 2, 3 and 4 of profile 2 is evident. At the same time, stick 5 and 6 have practically no estimated ice, identical to what was measured. Even more interesting is the increasing trend in intensity in profile 1 down slope, both in the measured and estimated values. The method described here overestimates the icing intensity by an average of 35 %.

During the second incident of icing, there was no pronounced difference in icing intensity between the east and the west side of the ridge for profiles 2 and 3, as it was observed in incident 1 (figure 11). Stick number 2 and 5 in profile 2 show an ice intensity of 0.036 Kg m^{-1} hr^{-1} and 0.029 Kg m^{-1} hr^{-1}, respectively, while the intensity at stick number 9 and 13 in profile 3 is

shown to be 0.030 Kg m^{-1} hr^{-1} and 0.033 Kg m^{-1} hr^{-1}, respectively. It should be mentioned here that the measured data from stick number 6 in profile 2 is missing in the second incident. Both profile 2 and 3 show maximum ice growth on the edge of the mountain ridge represented by stick 3 and 10, with ice growth of 0.054 Kg m^{-1} hr^{-1} and 0.065 Kg m^{-1} hr^{-1}, respectively. In addition, profile 1 shows no clear trend in ice accumulation with increasing height, varying from 0.029 Kg m^{-1} hr^{-1} at stick 8 to 0.054 Kg m^{-1} hr1 at stick3.
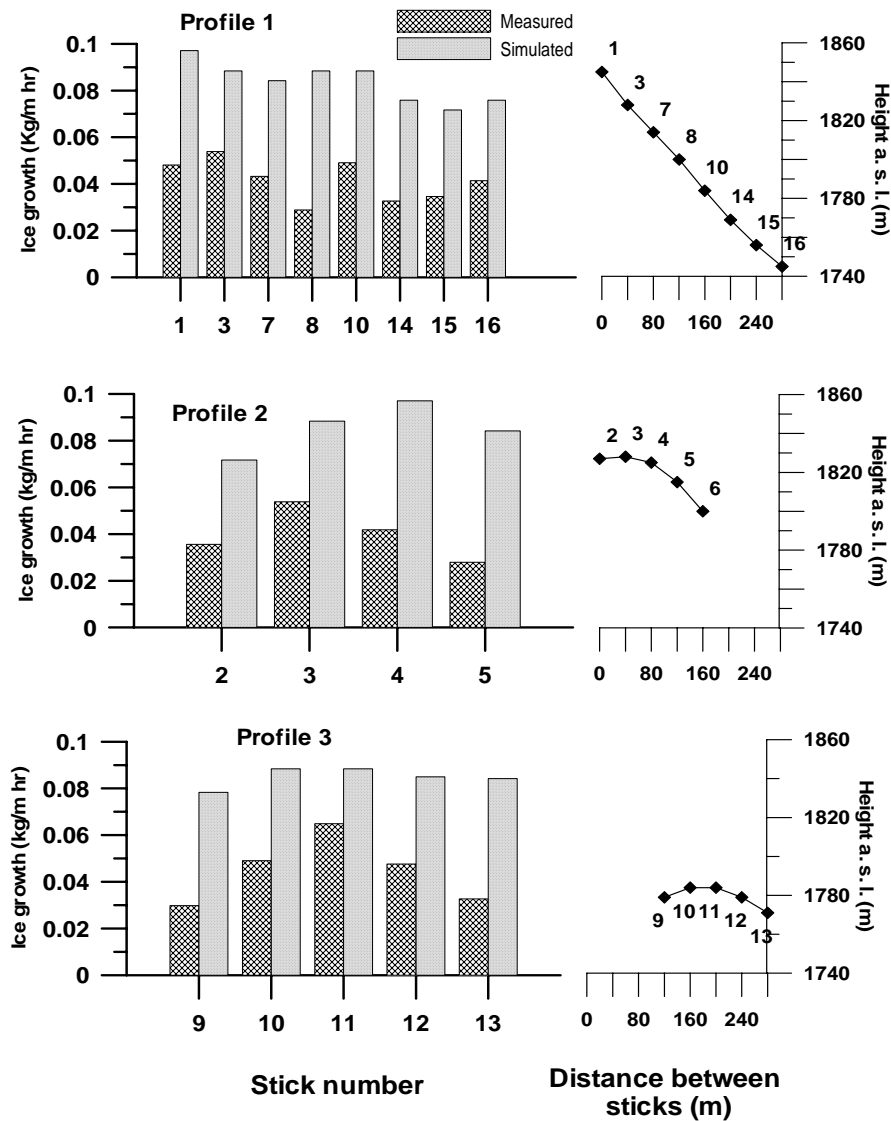

Figure 11. Plot of measured and estimated ice growth rate on each stick in the terrain during icing incident 2. Locations of the sticks related to height and horizontal distance is plotted to the left.

89

Observations indicate that the "diameter" of the ice vane decreases with time (Figure 4). Thus, the icing intensity also decreases with time, according to figure 1. The estimates of icing intensity performed in this study are based on the assumption that the cylinder diameter is a constant 3 cm throughout both icing incidents. An overestimate of ice intensity should therefore be expected in both icing incidents. The difference between measured and estimated icing intensity should also be expected to increase with increasing accumulated ice load on the sticks. This is confirmed in this study where an increase in accumulated ice loads from incident 1 (figure 10) to incident 2 (figure 11) gave a larger overestimate of icing intensity.

The simulated instantaneous icing intensity on the whole mountain peak is shown in figure 12a and 12b, for selected situations during the two simulation cases. This simulated icing intensity is indicating the variation in intensity relative to wind speed and wind direction.

For both cases calculated cloud base temperature of −6.7°C and cloud base height of 1505 m a.s.l, was chosen, resulting in a LWC of 0.22 (g/m3) at 1800 m a.s.l.

The fact that the simulated wind speed decreases slower than the ice growth rate might be explained by the variation in cloud liquid water content around the ridge. Icing onto the ground on the windward side of the ridge is a sink in the cloud LWC. In addition, the downward motion on the leeward side leads to evaporation.

The Median Volume Droplet diameter (MVD) has proven successful as the parameter to be applied when calculating the collision efficiency given the equations by Finstad et al. (1988b). No continuous measurement of the droplet spectrum or droplet concentration was performed in this study. Using mean volume droplet diameter would in most cases lead to an underestimate of the collision efficiency (Finstad et al, 1988b). In nature, two factors can be considered to reduce the difference between mean and median volume droplet size. First, the droplet size spectrum gets narrower, as the droplets grow by condensation of steady supersaturation (Rogers and Yau, 1989). Second, the spectrum is measured to have a majority of large droplets, giving a MVD more equal the mean volume droplet size (Schemenauer et al. 1980). The mean volume droplet size is therefore applied in this study, even if a slight overestimation should be expected in most cases.
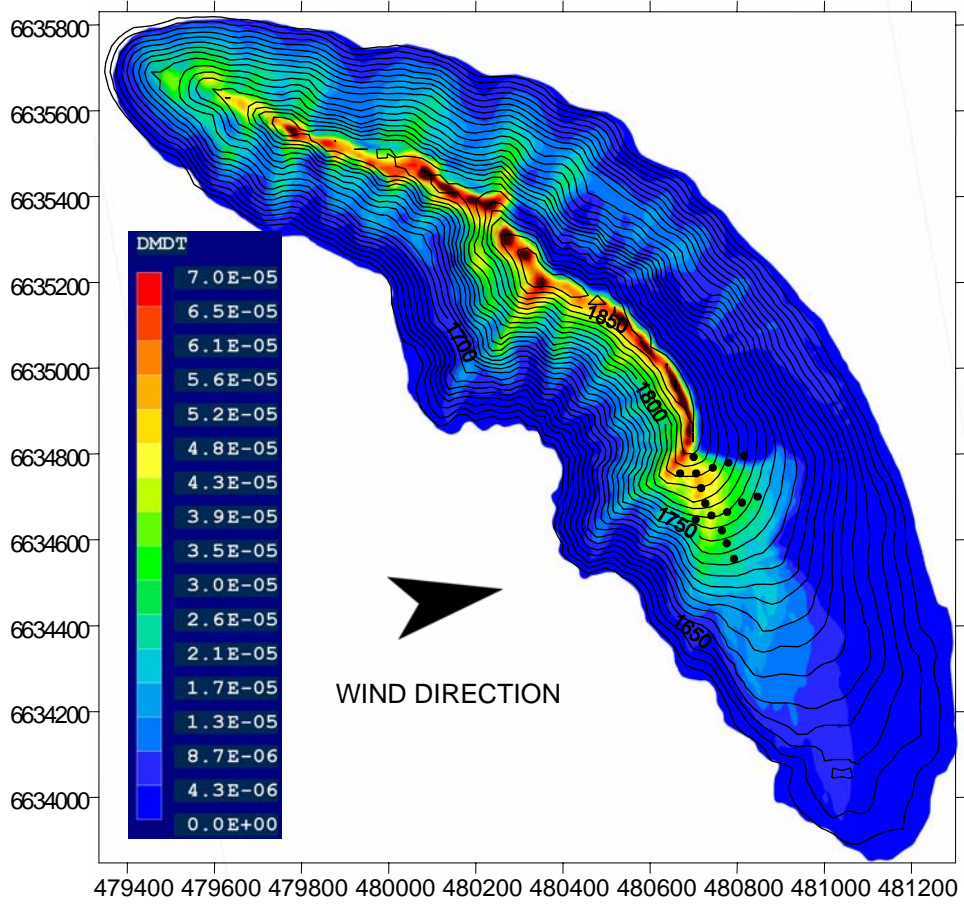
Figure 12a. Simulated icing intensity dM/dt (kg/s) in simulation case 1.
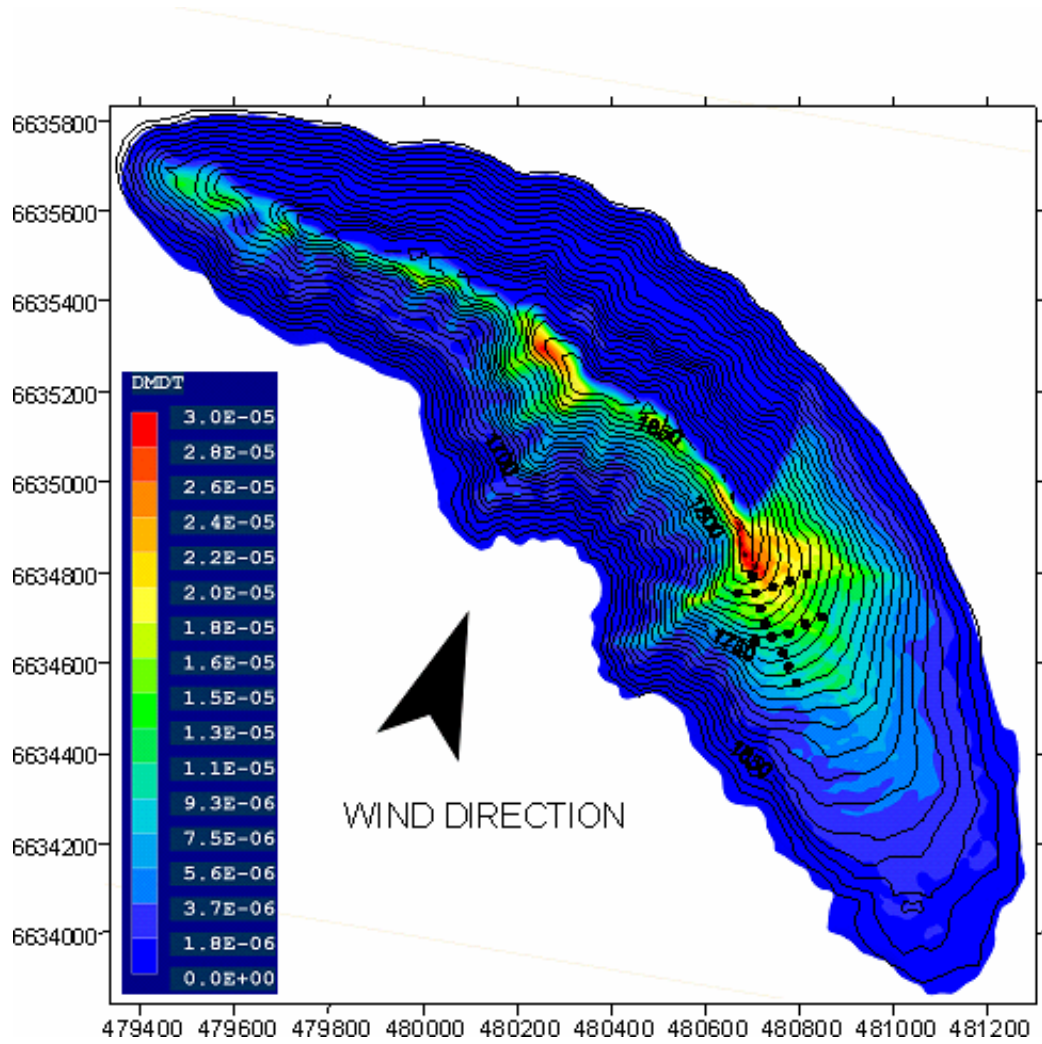LWC is 0.22 (g/m3) at 1800 m a.s.l. The scales on the axis are in meter.

Figure 12b. Simulated icing intensity, dM/dt (kg/s) in simulation case 2. LWC is 0.22 (g/m3) at 1800 m a.s.l. The scales on the axis are in meters.

4 DISCUSSION

The ice accumulations on the sticks at Gaustatoppen showed a strong dependence upon the actual location of the sticks. The main reason for this was the local variation in wind speed related to the topography. At wind directions perpendicular to the mountain ridge, the increase in wind speed over the ridge thereby causes an increase in ice load on the sticks located on the windward side of the ridge. This was verified by the first icing incident, both by measurement and simulation.

At wind directions parallel to the mountain ridge, there were no apparent zones showing increases or decreases in wind speed. Both measurements and simulations showed an increase in ice load on the sticks on the edge of the ridge, but no obvious relationship with height was identified.

The reason why the icing rate decreased rapidly with decreasing wind speed can be explained by equation 1. The wind speed and the LWC affect this equation in two ways. These parameters are both used directly in equation 1, but are also used to recalculate the collision coefficient α_1. It is easily shown that a reduction in wind speed or LWC will give a reduction in the collision efficiency.

5. CONCLUSION

The present measurements have shown that even small variations in the location of sticks around the ridge of a mountain peak can cause large variations in accreted ice onto these sticks. Existing methods for estimating design load for construction in such harsh environments are based upon the actual height of the site above sea level, together with climatologically data from synoptic weather stations or airports. To improve the estimates of in-cloud icing in the vicinity of the mountain peak several efforts may be undertaken. In this case, the application of micro scale numerical models, like computational fluid dynamics, to describe the wind field around the mountain peak, or measurements at the location for a short period of time, gave valuable information. The study of the icing around the building has shown that local sheltering might reduce the in cloud icing by up to 100 %. A basic understanding of the air flow around isolated mountain peaks is vital to

understanding how complex topography and changing wind direction strongly influence icing intensity.

REFERENCES

Cham inc., 2004, Phoenics 3.5 user guide

Drage, M. A. and Hauge G., 2004. Atmospheric icing in a coastal mountainous terrain – measurements and numerical simulations – a case study. Cold Regions Sc. and Tech., In Press.

Drage, M. A. and de Lange, T., 2005. Instrumentation for measuring atmospheric icing. Reports in meteorology and oceanography, Report No. 2-2005.

Finstad, K. J., Lozowzki, E. P. and Gates, E. M., 1988a. A computational investigation of water droplet trajectories. J. Atmos. Oceanic Technol. Vol 5. 160 – 170.

Finstad, K. J., Lozowzki, E. P. and Makkonen, L., 1988b. On the median volume diameter approximation for droplet collision efficiency. J. Atmos. Sci. Vol 45. 4008 – 4012.

Finstad, K., Fikke, S. M., and Ervik M., 1988c. Meteorological and cloud physical observations of atmospheric icing events on Gaustatoppen. Proceeding 4th International Workshop on Atmospheric Icing of Structures, 61 - 64.

Gjessing, Y. T., Skartveit, A., Utaaker, K., 1990. Vurdering av sikt- og vindforhold på Hurumåsen. Meteorological Report Series University of Bergen. Nr. 1, 1 – 49.

Harstveit, K., 2002. Using routine meteorological data from airfields to produce a map of ice risk zones in Norway. Proceeding 10th International Workshop on Atmospheric Icing of Structures, CD: Session 8-1.

Makkonen, L. and Stallabras, J. R., 1987. Experiments on the cloud droplet collision efficiency of cylinders, J. of Clim. Appl. Meteor., 26: 1406 – 1411.

Makkonen, L. and Ahti, K. 1995. Climatic mapping of ice loads based on airport weather observations, Atmos. Res., 36: 185 – 193.

Makkonen, L., 2000. Models for the growth of rime, glaze, icicles and wet sno won structures. Phil. Trans. Roy. Soc., Nr. 1776, Vol. 358 2913 – 2939.

Sundin, E. and Makkonen, L. 1998. Ice loads on a lattice tower estimated by weather station data. J. Applied Meteorology, Vol. 37(5), 523 – 529.

Raastad, H., 1958. Probes icing on overhead lines. Electric light and power, 42 – 51.

Rogers, R. R. and Yau, M. K., 1989. A short course in cloud physics, Pergamon Press.

Schemenauer, R. E., Macpherson, J. I., Isaac, G. A., and Strapp, J. W., 1980, Canadian participation in HIPLEX 1979. Report APRB 110 P 34, Atmospheric Environment Service, Environment Canada, 206 pp.

Stull, R. B., 1988. An introduction to boundary layer meteorology. Kluwer Academic Publishers.

Versteeg, H.K., Malalasekera, W., 1995 An introduction to computational fluid dynamics – The finite volume method, Longman Scientific& Technical

Yakhot, V., Orszag, S.A., Thangam, S., Gatski, T.B., Speziale, V.G., 1992, Development of turbulence models for shear flows by a double expansion technique, Phys. Fluids A, Vol. 4, no. 7, pp. 1510-1520